methods; however, of the semi-empirical methods, MNDO gave less satisfactory agreement for the bond lengths. We also note that molecular mechanics methods may give false minima as we have previously shown for this type of molecule (Badejo, Karaman, Pinkerton & Fry, 1990), hence the current MMX calculations use the solid-state structure as input to give results for comparison purposes only. The most important differences between the solid-state structure and the calculated ones concern the geometry associated with C9. This is perhaps not unexpected as the hydroxyl group, O15, attached to C9 is involved in hydrogen bonding in the solid (see above) which would be expected to perturb the geometry at C9 compared to the calculated gas-phase structures. The discrepancies relating to the geometry at O10 may also be interpreted in this way; however, there is certainly a contribution from the poor treatment of conjugated systems inherent in the molecular mechanics calculations. All of the calculations showed the energy minimum to be rather flat with respect to the conformation of the seven-membered ring, thus the discrepancies and the variation in the discrepancies for the torsion angles in this ring may be attributed to packing forces and/or uncertainties in the theoretical values.

All methods of calculation give similar heats of formation and dipole moments (Table 5). The weakness of the hydrogen bond is manifested in the similarity of the heat of formation calculated for the X-ray structure compared to that for the gas-phase molecule.

Table 5. *Heats of formation and dipole moments calculated for* (1)

Geometry	MNDO	AM1	PM3	MMX
Gas-phase optimized				
ΔH_f^0 (kcal mol⁻¹)*	28·2	33·9	29·7	28·3
μ (D)‡	1·41	1·27	1·39	1·85
X-ray optimized†				
ΔH_f^0 (kcal mol⁻¹)*	30·3	34·5	30·9	
μ (D)‡	1·43	1·40	1·32	

* 1 cal = 4·184 J.
† Optimization of the X-ray structure was done by forcing the torsion angles while all other parameters were optimized.
‡ 1 D ≃ 3·33564 × 10⁻³⁰ C m.

References

BADEJO, I. T., KARAMAN, R. & FRY, J. L. (1989). *J. Org. Chem.* **54**, 4591–4596.
BADEJO, I. T., KARAMAN, R., LEE, N. W. I., LUTZ, E. C., MAMANTA, M. T. & FRY, J. L. (1989). *J. Chem. Soc. Chem. Commun.* pp. 566–567.
BADEJO, I. T., KARAMAN, R., PINKERTON, A. A. & FRY, J. L. (1990). *J. Org. Chem.* **55**, 4327–4332.
BURKERT, U. & ALLINGER, N. L. (1982). *Molecular Mechanics*, ACS Monograph 177. Washington, DC: American Chemical Society.
DEWAR, M. J. S. & THIEL, W. (1977). *J. Am. Chem. Soc.* **99**, 4899–4907.
DEWAR, M. J. S., ZOEBISCH, E. G., HEALY, E. F. & STEWART, J. J. P. (1985). *J. Am. Chem. Soc.* **107**, 3902–3909.
FRENZ, B. A. (1978). *The Enraf–Nonius CAD-4 SDP – A Real Time System for Concurrent X-ray Data Collection and Crystal Structure Solution. In Computing in Crystallography*, edited by H. SCHENK, R. OLTHOF-HAZEKAMP, H. VAN KONINGSVELDT & G. C. BASSI, pp. 64–71. Delft Univ. Press.
JOHNSON, C. K. (1971) *ORTEPII.* Report ORNL-3794, revised. Oak Ridge National Laboratory, Tennessee, USA.
KARAMAN, R., BADEJO, I. T. & FRY, J. L. (1989). *J. Am. Chem. Soc.* **111**, 6450–6451.
Serena Software (1987). *MMX.* Version 87.2 from QCPE 395. Serena Software, Bloomington, Indiana, USA.
Serena Software (1989). *PCMODEL.* Version 1.3. Molecular modelling software. Serena Software, Bloomington, Indiana, USA.
STEWART, J. J. P. (1989). *J. Comput. Chem.* **10**, 209–220, 221–264.
THOMAS, R. & COPPENS, P. (1972). *Acta Cryst.* **B28**, 1800–1806.

Structures of Two Spiro[cyclopropane-1,3′-indoline]-*cis,syn*-1,3-dimethyluracil Cyclobutane Photodimers

BY THOMAS L. GROY,* SANG-TAE KIM AND SETH D. ROSE

Department of Chemistry, Arizona State University, Tempe, Arizona 85287-1604, USA

Abstract. (1) 4a-(Spiro[cyclopropane-1,3′-indolin]-2′-yl)-1,3,6,8-tetramethyl-4a,4b,8a,8b-tetracyclobuta-[1,2-*d*:4,3-*d*′]dipyrimidine-2,4,5,7(1*H*,3*H*,6*H*,8*H*)-tet-raone, $C_{22}H_{25}N_5O_4$, $M_r = 423·52$, monoclinic, $P2_1/c$, $a = 7·868$ (4), $b = 14·167$ (4), $c = 18·340$ (6) Å, $\beta = 92·69$ (4)°, $V = 2042$ (1) Å³, $Z = 4$, $D_m = 1·37$, $D_x = $

1·38 g cm^{-3}, λ(Mo $K\alpha$) = 0·71073 Å, μ(Mo $K\alpha$) = 0·91 cm^{-1}, F(000) = 896, T = 298 K, R = 0·0548 for 2868 observed data [$F_o > 3\sigma(F_o)$] of 5805 unique data collected. (2) $C_{22}H_{25}N_5O_4$, M_r = 423·52, orthorhombic, $Pna2_1$, a = 22·856 (12), b = 7·785 (4), c = 11·604 (3) Å, V = 2065 (1) Å^3, Z = 4, D_m = 1·36, D_x = 1·36 g cm^{-3}, λ(Mo $K\alpha$) = 0·71073 Å, μ(Mo $K\alpha$) = 0·90 cm^{-1}, F(000) = 896, T = 298 K, R = 0·0808 for 2172 observed data [$F_o > 3\sigma(F_o)$] of 4405 unique data collected. While differing only in configuration at the indoline C atom between the cyclobutyl group of the dimer and the N atom of the indoline, these two compounds exhibit markedly different dimer splitting efficiencies upon photochemical excitation of the indoline chromophore. For a given solvent, the splitting efficiency for (1) is twice that of (2).

Introduction. Exposure of DNA to ultraviolet-B radiation (280–320 nm) results in the formation of cyclobutane-type pyrimidine dimers in DNA. The presence of pyrimidine dimers in DNA has been associated with mutation, cell death and cellular transformation (Harm, 1980). Pyrimidine dimers are repaired by DNA photolyases (Sancar & Sancar, 1988), which utilize near-UV and visible light to regenerate the pyrimidines. The DNA photolyases may achieve dimer splitting by photoinitiated electron transfer from an enzyme-bound sensitizer to the dimer (Jordan & Jorns, 1988; Okamura, Sancar, Heelis, Hirata & Mataga, 1989; Pac & Ishitani, 1988).

Synthetic model compounds consisting of an indole ring covalently linked to a dimer have proved to be useful for mechanistic studies of dimer splitting (Kim, Hartman & Rose, 1990; Kim & Rose, 1988, 1990; Kim, Young, Goodman, Forrest, Hartman & Rose, 1990; Young, Kim, Van Camp, Hartman & Rose, 1988; Hartman, Van Camp & Rose, 1987; Van Camp, Young, Hartman & Rose, 1987). In these systems, absorption of light results in electron donation from photo-excited indole to a dimer, followed by splitting of the dimer radical anion.

Two diastereomeric compounds, (1) and (2), in which a pyrimidine dimer is directly attached to an indoline ring, have been prepared to examine intramolecularly photosensitized dimer splitting (Kim & Rose, 1991). These two compounds, differing only in configuration at the indoline C atom between the cyclobutyl group of the dimer and the N atom of the indoline, exhibited quite different dimer splitting efficiencies upon photochemical excitation of the indoline chromophore. Their stereochemistry, however, could not be assigned unambiguously by spectroscopic methods.

This paper reports the crystal structures of two cis,syn-1,3-dimethyluracil photodimers with a co-

valently linked spiro[cyclopropane-1,3'-indoline], (1) and (2).

(1)   (2)
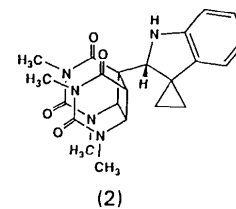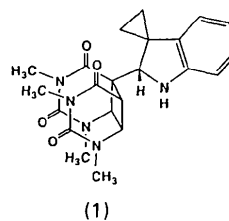
Experimental. *Preparation of cis,syn-1,3-dimethyluracil photodimers with a covalently linked spiro[cyclopropane-1,3'-indoline], (1) and (2).* The preparation of these compounds will be reported elsewhere (Kim & Rose, 1991). Single crystals of racemic (1) from ethyl acetate/methanol and of racemic (2) from ethyl acetate/ethanol were obtained at room temperature. Density was measured by flotation in aqueous cadmium chloride.

Structure determination. A Siemens $R3m/V$ 2000 diffractometer was used for data collection. Cell parameters for each crystal were refined by least squares on 25 reflections in the 2θ range 3·5–15·0°. Intensities were collected with Mo $K\alpha$ radiation (λ = 0·71073 Å) in the range 3·5 ≤ 2θ ≤ 50·0° using the ω-scan technique. The data were corrected for Lorentz and polarization effects, but no absorption correction was applied. Data with $F_o \geq 3\sigma(F_o)$ were considered observed [2868 of 5805 unique data for (1), R_{int} = 0·0203; 2172 of 4405 unique data for (2), R_{int} = 0·0460]. Both structures were solved by direct methods (*SHELXTL-Plus*; Sheldrick, 1990) on a DEC MicroVAX 2000 computer. The structures were refined by full-matrix least squares on F. H atoms were added in idealized positions and refined as atoms riding on their bonding partners. For (1), the final conventional R = 0·0548 and wR = 0·0612 where w = 1·000/[$\sigma^2(F)$ + 0·000138(F^2)]. For (2), the final conventional R = 0·0808 and wR = 0·0522 where w = 1·000/[$\sigma^2(F)$ + 0·000103(F^2)]. The largest peaks in final difference maps were 0·35 e Å^{-3} for (1) and 0·33 e Å^{-3} for (2). The ranges of hkl were -11 to 11, 0 to 19, 0 to 25, respectively, for (1) and 0 to 36, 0 to 12, 0 to 18, respectively, for (2). The final (Δ/σ)$_{max}$ values were 0·002 for both structures. Three standard reflections ($0\bar{2}1$, $1\bar{1}1$ and $00\bar{2}$) for (1), and (012, 110 and 101) for (2), were collected every 47 reflections and indicated no discernible degradation of either compound (variation in standard intensities < 1%). The high R value for (2) was due to a larger fraction of the data having low intensity, as expected for the higher-symmetry space group [44% of data <4$\sigma(F)$ for (2), whereas 29% of data <4$\sigma(F)$ for (1)]. Both structure determinations, as well as the production of the plots, were performed

using the *SHELXTL-Plus* package. Atomic scattering factors were also from the *SHELXTL-Plus* package.

Discussion. The final atomic parameters with their estimated standard deviations are listed in Table 1.* Selected bond lengths and angles with the associated estimated standard deviations appear in Table 2. A view of both molecules, together with the atom-labeling scheme, is given in Fig. 1. Stereoviews of the unit cells of (1) and (2) are shown in Figs. 2 and 3, respectively. The bond lengths and angles in the pyrimidine dimer portion of both (1) and (2) are

---

* Lists of structure factors, anisotropic thermal parameters, complete bond lengths and angles and H-atom parameters have been deposited with the British Library Document Supply Centre as Supplementary Publication No. SUP 53986 (48 pp.). Copies may be obtained through The Technical Editor, International Union of Crystallography, 5 Abbey Square, Chester CH1 2HU, England.
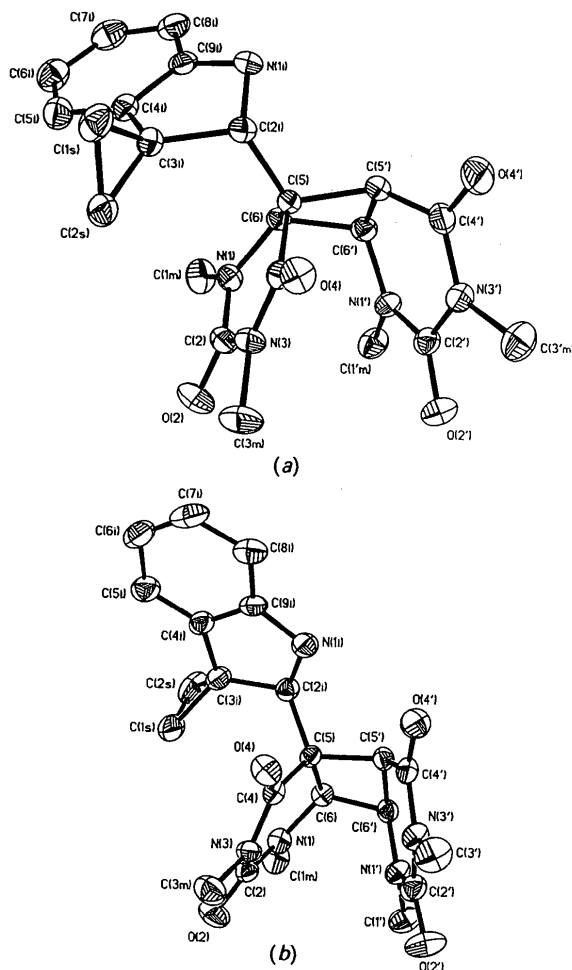

Fig. 1. (a) Perspective view of (1) and (b) of (2), with atom-labeling schemes. H atoms are omitted for clarity. Thermal ellipsoids are depicted at the 30% probability level.

Table 1. *Atomic coordinates* ($\times 10^4$) *and equivalent isotropic displacement coefficients* ($\text{Å}^2 \times 10^3$)

U_{eq} is defined as one third of the trace of the orthogonalized U_{ij} tensor.

	x	y	z	U_{eq}
Compound (1)				
N(1)	9840 (3)	4681 (1)	2821 (1)	37 (1)
C(2)	8840 (3)	5386 (2)	2559 (1)	40 (1)
N(3)	7162 (3)	5153 (1)	2323 (1)	39 (1)
C(4')	6422 (3)	4276 (2)	2376 (1)	34 (1)
C(5)	7542 (3)	3460 (2)	2628 (1)	32 (1)
C(6)	9439 (3)	3705 (2)	2666 (1)	34 (1)
N(1')	9529 (3)	4001 (2)	1312 (1)	39 (1)
C(2')	8175 (3)	4158 (2)	849 (1)	40 (1)
N(3')	6828 (3)	3498 (2)	831 (1)	42 (1)
C(4')	6660 (3)	2779 (2)	1326 (2)	45 (1)
C(5')	7917 (3)	2792 (2)	1961 (1)	39 (1)
C(6')	9630 (3)	3297 (2)	1879 (1)	38 (1)
N(1*i*)	7856 (3)	2213 (2)	3592 (1)	46 (1)
C(2*i*)	6764 (3)	2985 (2)	3299 (1)	38 (1)
C(3*i*)	6651 (3)	3625 (2)	3970 (1)	39 (1)
C(4*i*)	8196 (3)	3402 (2)	4428 (1)	41 (1)
C(5*i*)	8948 (4)	3860 (2)	5026 (2)	56 (1)
C(6*i*)	10375 (4)	3459 (2)	5382 (2)	63 (1)
C(7*i*)	11018 (4)	2621 (3)	5133 (2)	62 (1)
C(8*i*)	10275 (4)	2148 (2)	4536 (2)	53 (1)
C(9*i*)	8854 (3)	2558 (2)	4190 (1)	41 (1)
O(2)	9313 (3)	6210 (1)	2532 (1)	64 (1)
O(2')	8089 (3)	4832 (1)	436 (1)	57 (1)
O(4)	4919 (2)	4153 (1)	2219 (1)	49 (1)
O(4')	5535 (3)	2192 (2)	1264 (1)	68 (1)
C(1*m*)	11541 (3)	4901 (2)	3130 (2)	59 (1)
C(1'*m*)	11072 (3)	4569 (2)	1212 (2)	54 (1)
C(3*m*)	6075 (4)	5935 (2)	2051 (2)	64 (1)
C(3'*m*)	5498 (4)	3622 (2)	252 (2)	61 (1)
C(2*s*)	5763 (4)	4569 (2)	3995 (2)	53 (1)
C(1*s*)	4983 (4)	3728 (2)	4350 (2)	56 (1)
Compound (2)				
N(1)	3124 (2)	3227 (5)	5000	47 (1)
C(2)	2717 (2)	2130 (6)	4636 (5)	44 (2)
N(3)	2911 (1)	503 (4)	4236 (4)	43 (1)
C(4)	3464 (2)	−169 (6)	4389 (5)	41 (1)
C(5)	3934 (2)	1023 (5)	4828 (5)	36 (1)
C(6)	3742 (2)	2931 (5)	4855 (5)	40 (1)
N(1')	3686 (2)	3291 (5)	2680 (5)	47 (1)
C(2')	3676 (2)	2079 (6)	1834 (6)	53 (2)
N(3')	4027 (2)	603 (5)	1971 (4)	47 (1)
C(4')	4408 (2)	330 (6)	2849 (5)	43 (1)
C(5')	4374 (2)	1551 (5)	3839 (5)	39 (1)
C(6')	4051 (2)	3266 (6)	3684 (5)	41 (1)
C(1*m*)	2938 (2)	4906 (6)	5457 (6)	70 (2)
C(3*m*)	2456 (2)	−671 (7)	3798 (6)	68 (2)
O(2)	2195 (1)	2433 (4)	4663 (5)	71 (1)
O(4)	3570 (1)	−1661 (4)	4166 (4)	57 (1)
C(1')	3383 (2)	4915 (6)	2436 (6)	72 (2)
C(3')	3999 (3)	−711 (7)	1058 (6)	72 (2)
O(2')	3379 (2)	2216 (5)	971 (5)	81 (2)
O(4')	4742 (1)	−906 (4)	2877 (4)	60 (1)
N(1*i*)	4638 (2)	−1137 (5)	5591 (5)	56 (1)
C(2*i*)	4250 (2)	292 (6)	5886 (5)	45 (2)
C(3*i*)	3890 (2)	−392 (6)	6914 (5)	52 (2)
C(4*i*)	4156 (2)	−2074 (6)	7194 (5)	48 (2)
C(5*i*)	4043 (2)	−3194 (7)	8083 (6)	63 (2)
C(6*i*)	4354 (3)	−4756 (7)	8114 (7)	76 (2)
C(7*i*)	4749 (2)	−5165 (7)	7281 (7)	72 (2)
C(8*i*)	4876 (2)	−4048 (7)	6382 (6)	61 (2)
C(9*i*)	4576 (2)	−2474 (6)	6365 (5)	47 (2)
C(1*s*)	3238 (2)	−149 (9)	7071 (6)	84 (2)
C(2*s*)	3655 (3)	785 (8)	7828 (6)	82 (2)

generally similar to those found in the same *cis,syn*-type pyrimidine photodimers (Adman & Jensen, 1970; Camerman & Camerman, 1970; Konnert, Gibson, Karle, Khattak & Wang, 1970; Groy, Kim & Rose, 1991). The cyclobutyl ring in (1) is more folded than in (2), with a torsional angle of 16·8° about C(5)—C(6) and C(5')—C(6'), compared to 14·7° in (2). These angles can be compared to those

Table 2. *Bond lengths* (Å) *and bond angles* (°)

Compound (1)

C(5)—C(6)	1·531 (3)	C(5)—C(5')	1·586 (4)
C(6)—C(6')	1·570 (4)	C(5')—C(6')	1·539 (4)
N(1i)—C(2i)	1·477 (3)	N(1i)—C(9i)	1·405 (3)
C(2i)—C(3i)	1·534 (4)	C(3i)—C(4i)	1·479 (4)
C(3i)—C(2s)	1·510 (4)	C(3i)—C(1s)	1·523 (4)
C(4i)—C(5i)	1·384 (4)	C(4i)—C(9i)	1·382 (4)
C(5i)—C(6i)	1·393 (4)	C(6i)—C(7i)	1·378 (5)
C(7i)—C(8i)	1·388 (4)	C(8i)—C(9i)	1·387 (4)
C(2s)—C(1s)	1·503 (4)		
C(6)—C(5)—C(5')	87·4 (2)	C(5)—C(6)—C(6')	90·6 (2)
C(5)—C(5')—C(6')	89·6 (2)	C(6)—C(6')—C(5')	87·7 (2)
C(2i)—N(1i)—C(9i)	108·7 (2)	C(5)—C(2i)—C(3i)	111·4 (2)
C(5)—C(2i)—C(3i)	114·8 (2)	N(1i)—C(2i)—C(3i)	101·6 (2)
C(2i)—C(3i)—C(4i)	104·6 (2)	C(2i)—C(3i)—C(2s)	126·3 (2)
C(4i)—C(3i)—C(2s)	122·8 (2)	C(2i)—C(3i)—C(1s)	120·5 (2)
C(4i)—C(3i)—C(1s)	117·6 (2)	C(2s)—C(3i)—C(1s)	59·4 (2)
C(3i)—C(4i)—C(5i)	131·2 (3)	C(3i)—C(4i)—C(9i)	108·4 (2)
C(5i)—C(4i)—C(9i)	120·2 (2)	C(4i)—C(5i)—C(6i)	119·1 (3)
C(5i)—C(6i)—C(7i)	119·8 (3)	C(6i)—C(7i)—C(8i)	122·0 (3)
C(7i)—C(8i)—C(9i)	117·4 (3)	N(1i)—C(9i)—C(4i)	110·1 (2)
N(1i)—C(9i)—C(8i)	128·4 (3)	C(4i)—C(9i)—C(8i)	121·6 (2)
C(3i)—C(2s)—C(1s)	60·7 (2)	C(3i)—C(1s)—C(2s)	59·9 (2)

Compound (2)

C(5)—C(6)	1·549 (6)	C(5)—C(5')	1·580 (7)
C(6)—C(6')	1·553 (8)	C(5')—C(6')	1·536 (6)
N(1i)—C(2i)	1·462 (6)	N(1i)—C(9i)	1·382 (7)
C(2i)—C(3i)	1·545 (8)	C(3i)—C(4i)	1·479 (7)
C(3i)—C(1s)	1·514 (7)	C(3i)—C(2s)	1·502 (9)
C(4i)—C(5i)	1·375 (8)	C(4i)—C(9i)	1·394 (8)
C(5i)—C(6i)	1·409 (8)	C(6i)—C(7i)	1·360 (10)
C(7i)—C(8i)	1·389 (9)	C(8i)—C(9i)	1·405 (7)
C(1s)—C(2s)	1·486 (9)		
C(6)—C(5)—C(5')	86·9 (3)	C(5)—C(6)—C(6')	90·8 (4)
C(5)—C(5')—C(6')	90·3 (3)	C(6)—C(6')—C(5')	88·3 (4)
C(2i)—N(1i)—C(9i)	111·0 (4)	C(5)—C(2i)—N(1i)	112·3 (5)
C(5)—C(2i)—C(3i)	119·7 (4)	N(1i)—C(2i)—C(3i)	104·0 (4)
C(2i)—C(3i)—C(4i)	104·8 (4)	C(2i)—C(3i)—C(1s)	125·1 (5)
C(4i)—C(3i)—C(1s)	119·2 (5)	C(2i)—C(3i)—C(2s)	121·7 (4)
C(4i)—C(3i)—C(2s)	122·2 (5)	C(1s)—C(3i)—C(2s)	59·0 (4)
C(3i)—C(4i)—C(5i)	130·5 (5)	C(3i)—C(4i)—C(9i)	109·2 (5)
C(5i)—C(4i)—C(9i)	120·3 (5)	C(4i)—C(5i)—C(6i)	118·2 (6)
C(5i)—C(6i)—C(7i)	121·2 (6)	C(6i)—C(7i)—C(8i)	121·8 (5)
C(7i)—C(8i)—C(9i)	117·0 (5)	N(1i)—C(9i)—C(4i)	110·5 (4)
N(1i)—C(9i)—C(8i)	128·0 (5)	C(4i)—C(9i)—C(8i)	121·5 (5)
C(3i)—C(1s)—C(2s)	60·1 (4)	C(3i)—C(2s)—C(1s)	60·9 (4)

of 6-methyluracil *cis,syn*-photodimer, in which the torsional angle is 16·5° (Gibson & Karle, 1971). In 1,3-dimethyluracil *cis,syn*-photodimers with a covalently linked indole, the torsional angles were 16·9 and 15·4° (Groy, Kim & Rose, 1991). The average of the dihedral angles between the planes determined by C(4)—C(5)—C(5') and C(5)—C(5')—C(4') and between the planes determined by N(1)—C(6)—C(6') and C(6)—C(6')—N(1'), which is a measure of the twist of the pyrimidine rings relative to each other, is 24·8° in (1), whereas the average in (2) is 22·4°.

The dihedral angle between the planes determined by N(1i)—C(2i)—C(3i) and C(4i)—C(5i)—C(6i)—C(7i)—C(8i)—C(9i), which is a measure of the non-planarity of the indoline ring, is 22·7 and 6·5° for (1) and (2) respectively. Thus (1) exhibits greater non-planarity of the indoline ring than does (2), and the deviation of the C(2i) atom from the phenyl ring plane is −0·3184 Å in (1) and 0·0929 Å in (2). The cyclopropyl ring in each compound is nearly at a right angle to the indoline ring, the dihedral angles

between the C(1s)—C(2s)—C(3i) plane and the C(4i)—C(5i)—C(6i)—C(7i)—C(8i)—C(9i) plane being 83·1 and 91·2° for (1) and (2), respectively. In addition, the torsional angle C(2s)—C(3i)—C(4i)—C(9i) is 120° in (1) and −150·4° in (2). That is, the cyclopropyl ring in (1) is essentially above the plane of the indoline ring, whereas the cyclopropyl ring in (2) is virtually bisected by the indoline ring. The π-like orbitals of the cyclopropyl group of (2) are thus better oriented than those of (1) for overlap with the π system of the neighboring phenyl ring [*i.e.*, the *p* orbitals of C(3i) and C(4i) are parallel]. Altered ring-current effects experienced by C(2i) due to its deviation from the plane of the phenyl ring as well as electronic effects of the phenyl ring exerted through the cyclopropyl orbital system at C(3i) may be responsible for the significantly farther downfield shift (δ 71·14 *vs* 64·46 p.p.m.) of the C(2i) resonance observed in the ^{13}C NMR spectrum (Me$_2$SO-d_6) of (2) compared to (1).

Both compounds exhibit dimer splitting efficiencies that are highly dependent on solvent polarity (Kim & Rose, 1991), but (1) splits twice as efficiently as (2) in a given solvent. This may be a consequence of a difference in ability of the ground-state dimer and photochemically excited indoline portions of each molecule to interact. For example,
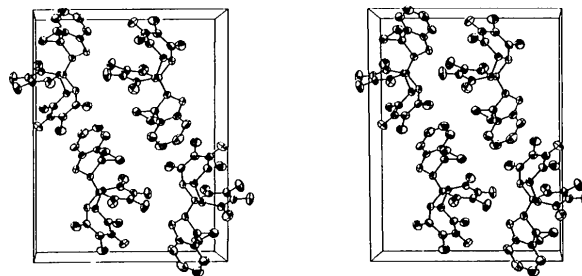

Fig. 2. Stereoview of the unit cell of (1) as viewed down the *a* axis, with *b* axis to the right and *c* axis down. H atoms are omitted for clarity.
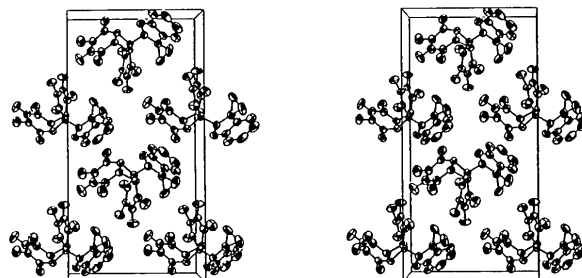

Fig. 3. Stereoview of the unit cell of (2) as viewed down the *b* axis, with *a* axis up and *c* axis to the left. H atoms are omitted for clarity.

the dihedral angle between π orbitals that may have to interact [*i.e.*, those spanning C(3*i*)—C(4*i*)—C(9*i*)—N(1*i*) and spanning C(5)—C(4)—N(3)—C(2)] is 133·4° in (1) and 67·8° in (2). If the predominant solution conformations of (1) and (2) resemble the conformations in the crystal, then this stereoelectronic effect might be responsible for differences in photosplitting efficiencies of (1) and (2).

References

ADMAN, E. & JENSEN, L. H. (1970). *Acta Cryst.* B26, 1326–1334.

CAMERMAN, N. & CAMERMAN, A. (1970). *J. Am. Chem. Soc.* 92, 2523–2527.

GIBSON, J. W. & KARLE, I. L. (1971). *J. Cryst. Mol. Struct.* 1, 115–121.

GROY, T., KIM, S. T. & ROSE, S. D. (1991). *Acta Cryst.* C47, 1287–1290.

HARM, W. (1980). *Biological Effects of Ultraviolet Radiation*, pp. 140–157. London: Cambridge Univ. Press.

HARTMAN, R. F., VAN CAMP, J. R. & ROSE, S. D. (1987). *J. Org. Chem.* 52, 2684–2689.

JORDAN, S. P. & JORNS, M. S. (1988). *Biochemistry*, 27, 8915–8923.

KIM, S. T., HARTMAN, R. F. & ROSE, S. D. (1990). *Photochem. Photobiol.* 52, 789–794.

KIM, S. T. & ROSE, S. D. (1988). *Photochem. Photobiol.* 47, 725–729.

KIM, S. T. & ROSE, S. D. (1990). *J. Phys. Org. Chem.* 3, 581–586.

KIM, S. T. & ROSE, S. D. (1991). *J. Photochem. Photobiol. B.* Submitted.

KIM, S. T., YOUNG, T., GOODMAN, M. S., FORREST, C., HARTMAN, R. F. & ROSE, S. D. (1990). *Res. Trends Photochem. Photobiol.* 1, 81–87.

KONNERT, J., GIBSON, J. W., KARLE, I. L., KHATTAK, M. N. & WANG, S. Y. (1970). *Nature (London)*, 227, 953–954.

OKAMURA, T., SANCAR, A., HEELIS, P. F., HIRATA, Y. & MATAGA, N. (1989). *J. Am. Chem. Soc.* 111, 5967–5969.

PAC, C. & ISHITANI, O. (1988). *Photochem. Photobiol.* 48, 767–785.

SANCAR, A. & SANCAR, G. B. (1988). *Annu. Rev. Biochem.* 57, 29–67.

SHELDRICK, G. M. (1990). *SHELXTL-Plus.* Siemens Analytical X-ray Instruments Inc., Madison, Wisconsin, USA.

VAN CAMP, J. R., YOUNG, T., HARTMAN, R. F. & ROSE, S. D. (1987). *Photochem. Photobiol.* 45, 365–370.

YOUNG, T., KIM, S. T., VAN CAMP, J. R., HARTMAN, R. F. & ROSE, S. D. (1988). *Photochem. Photobiol.* 48, 635–641.

Structure of 9-Benzyl-1,3-dimethyl-2,4,8-trioxo-1,3,6,7,9-pentahydro-1,3-diazino[2,1-*f*]purine

BY ZBIGNIEW KARCZMARZYK

Department of Chemistry, Agricultural and Teachers University, ul. 3 Maja 54, 08-110 Siedlce, Poland

JANINA KAROLAK-WOJCIECHOWSKA

Institute of General Chemistry, Technical University, ul. Żwirki 36, 90-924 Łódź, Poland

AND MACIEJ PAWŁOWSKI

Department of Pharmaceutical Chemistry, Medical Academy, ul. Skałeczna 10, Kraków, Poland

Abstract. $C_{17}H_{17}N_5O_3$, $M_r = 339\cdot35$, orthorhombic, *Pbca*, $a = 7\cdot521$ (1), $b = 38\cdot635$ (4), $c = 11\cdot008$ (1) Å, $V = 3198\cdot6$ (6) Å³, $Z = 8$, $D_m = 1\cdot40$ (2), $D_x = 1\cdot409$ g cm⁻³, $\lambda(Cu K\alpha) = 1\cdot54178$ Å, $\mu = 7\cdot88$ cm⁻¹, $F(000) = 1424$, $T = 293$ K, final $R = 0\cdot0514$ for 1157 observed reflections. The purine fused-ring system is planar. The six-membered 1,3-diazinone ring adopts a half-chair conformation. Theophylline skeletons show significant stacking with mean separation between molecular planes of 3·34 (4) Å.

Introduction. Theophylline, as natural methylxanthine, is a well known pharmacological agent of great therapeutic interest. The structure determination of 9-benzyl-1,3-dimethyl-2,4,8-trioxo-1,3,6,7,9-pentahydro-1,3-diazino[2,1-*f*]purine (I) is part of a larger X-ray and pharmacological study on tricyclic theophylline derivatives (Karolak-Wojciechowska & Pawłowski, 1990). The annelation of the six-membered lactam ring at the 7,8-position of theophylline changes the profile of its activity to neurosedative action, probably due to the chemical properties of the third lactam ring (Pawłowski, Drabczyńska, Gorczyca, Malec & Modzelewski, 1991). Incorporation of this ring allows us to expect a higher lipophility and a better absorption by the central nervous system. These pharmacological